Metal-Assisted Racemization of the Atropisomers of a 1,1′-Binaphthyl Skeleton via a *Syn* Transition State[1]

Michael T. Ashby,* Geetha N. Govindan, and Anthony K. Grafton

Contribution from the Department of Chemistry and Biochemistry, University of Oklahoma, Norman, Oklahoma 73019

*Received September 7, 1993. Revised Manuscript Received February 23, 1994**

Abstract: Δ/Λ-(δ/λ-1,1′-Biisoquinoline)bis(2,2′-bipyridine)ruthenium(II) bis(hexafluorophosphate) (**2**) exists as an ~3:1 mixture of its two diastereomeric forms in acetone solutions at 25 °C. The major isomer, (Δ,δ/Λ,λ)-**2**, crystallizes in the monoclinic space group $C2/c$ with $Z = 8$, $a = 29.12(1)$, $b = 18.593(7)$, and $c = 17.85(1)$ Å, $\beta = 127.81(4)°$, $R = 0.053$, and $R_w = 0.062$ at 25 °C. As expected, the 1,1′-biisoquinoline ligand is nonplanar, which is a result of a transannular steric interaction between H_8 and $H_{8'}$. Diastereomerically pure samples of **2** were found to isomerize rapidly in solution at room temperature in the absence of light to give a thermodynamic mixture of the two diastereomers. The rate data for the latter equilibrium at 80 °C are $K = 2.89$, $k(6a_{maj} \rightarrow 6a_{min}) = 12.7(3)$ s^{-1}, and $k(6a_{min} \rightarrow 6a_{maj}) = 36.6(9)$ s^{-1}. The activation parameters were determined in the temperature range of 50–90 °C: $\Delta H^{\ddagger}$ (maj→min) = 68.7 kJ mol^{-1}, $\Delta S^{\ddagger}$(maj→min) = −21 J K^{-1} mol^{-1}, $\Delta H^{\ddagger}$(min→maj) = 66.1 kJ mol^{-1}, and $\Delta S^{\ddagger}$(min→maj) = −38 J K^{-1} mol^{-1}. Spin saturation transfer (SST), spin inversion transfer (SIT), and two-dimensional exchange spectroscopy (2D EXSY) NMR experiments using **2** and its 2,2′-bipyridine-d_8 analogue demonstrate that the interconversion of the two diastereomers is the result of an intramolecular process of C_2 symmetry that does not change the *cis*/*trans* relationship between the 1,1′-biisoquinoline and 2,2′-bipyridine ligands. Irregular mechanisms that involve breaking just one of the ruthenium–isoquinoline bonds have been ruled out because the rate of isomerization of a water-soluble derivative of **2**, Δ/Λ-(δ/λ-1,1′-biisoquinoline)bis(2,2′-bipyridine)ruthenium(II) dichloride, is essentially the same in D_2O containing 1 M LiCl ($k(6a_{maj} \rightarrow 6a_{min}) = 5.7(2)$ s^{-1}) and 1 M DCl ($k(6a_{maj} \rightarrow 6a_{min}) = 7.1(1)$ s^{-1}) at 80 °C. We therefore conclude that interconversion of the two diastereoisomers of **2** takes place by a regular mechanism that involves atropisomerization of the η^2-1,1′-biisoquinoline ligand via a *syn* transition state.

Introduction

The high barrier to rotation about the σ-bond of 1,1′-binaphthyl and its derivatives gives rise to atropisomers.[2] In some cases, racemization of 1,1′-binaphthyl derivatives is kinetically facile at room temperature. For example, the parent compound has a half-life of ca. 10 h at 25 °C.[3] However, substitution of the C_2 and $C_{2'}$ positions of 1,1′-binaphthyl creates a nearly insurmountable barrier to rotation.[4] Indeed, this has been exploited in the development of several ancillary chiral ligand systems that have been employed in stoichiometric and catalytic chiral induction reactions.[5]

Two mechanisms have been proposed for racemization of the 1,1′-binaphthyl skeleton: (1) rotation about the σ-bond via an *anti* transition state, which brings X and $H_{8'}$ in close proximity to one another, and (2) rotation about the σ-bond via a *syn* transition state, which brings X and X′ and H_8 and $H_{8'}$ in close proximity to one another. It has been assumed that racemization

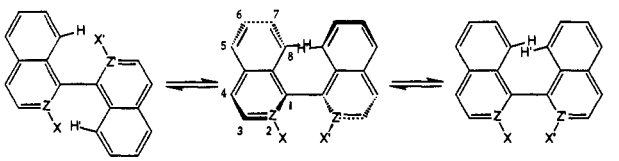

via the *anti* transition state represents the lower energy barrier. Molecular mechanics studies support this assumption.[6] Although the *anti* transition state is still generally believed to lie lower in energy than the *syn* transition state in most cases, a recent semiempirical molecular orbital study of the barriers to racemization of **1** (Z = Z′ = C) concludes that one derivative that was looked at (X = X′ = Br) actually prefers to racemize via the *syn* transition state.[7,8] The present study involves 1,1′-biisoquinoline, which does not bear substituents in the 2 and 2′ positions and, therefore, exhibits little resistance toward atropisomerization via the *anti* transition state. Coordination of 1,1′-biisoquinoline to kinetically inert metals should result in retardation of atropisomerization. We report here the kinetics and mechanism of the diastereomeric isomerization of the kinetically inert complex Δ/Λ-(δ/λ-1,1′-biisoquinoline)bis(2,2′-bipyridine)ruthenium(II), which may be viewed as a 1,1′-binaphthyl derivative (**1**, Z

(1) Presented in part at the 206th National Meeting of the American Chemical Society, Chicago, IL, Aug 22–27, 1993; INOR 1.

* Abstract published in *Advance ACS Abstracts*, April 15, 1994.

(2) Atropisomers are conformational isomers that are separable because of hindered rotation about a σ-bond.

(3) (a) Cooke, A. S.; Harris, M. M. *J. Chem. Soc. B* **1963**, 2365. (b) Colter, A. K.; Clements, L. M. *J. Phys. Chem.* **1964**, *68*, 651. (c) Kress, R. B.; Duesler, E. N.; Etter, M. C.; Paul, I. C.; Curtin, D. Y. *J. Am. Chem. Soc.* **1980**, *102*, 7709 and references therein.

(4) For example, 1,1′-dinaphthyl-2,2′-dicarboxylic acid is recovered unchanged from *N*-methylformamide heated to 175 °C for 8 h, and it decomposes without racemization in boiling ethylene glycol: Hall, D. M.; Turner, E. E. *J. Chem. Soc.* **1955**, 1242.

(5) See the following references for recent examples of asymmetric catalysis based upon 1,1′-binaphthyl systems. 1,1′-Binaphthalene-modified "twin-cornet" porphyrins (oxidation of alkenes to give epoxides): Naruta, Y.; Tani, F.; Ishihara, N.; Maruyama, K. *J. Am. Chem. Soc.* **1991**, *113*, 6865. Mikami, K.; Narisawa, S.; Shimizu, M.; Terada, M. *J. Am. Chem. Soc.* **1992**, *114*, 6566 and references therein. 2,2′-Diphosphino-1,1′-binaphthyl (kinetic resolution): Kitamura, M.; Tokunaga, M.; Noyori, R. *J. Am. Chem. Soc.* **1993**, *115*, 144 and references therein. Asymmetric epoxidation of alkenes with binaphthyl-bridged metallocenes: Halterman, R. L.; Ramsey, T. M. *Organometallics* **1993**, *12*, 2879.

(6) Gamba, A.; Rusconi, E.; Simonetta, M. *Tetrahedron* **1970**, *26*, 871. (b) Carter, R. E.; Liljefors, T. *Tetrahedron* **1976**, *32*, 2915. (c) Gustav, K.; Sühnel, J.; Wild, U. P. *Chem. Phys.* **1978**, *31*, 59. (d) Liljefors, T.; Carter, R. E. *Tetrahedron* **1978**, *34*, 1611. (e) Leister, D.; Kao, J. *J. Mol. Struct.* **1988**, *168*, 105. (f) Tsuzuki, S.; Tanabe, K.; Nagawa, Y.; Nakanishi, H. *J. Mol. Struct.* **1990**, *216*, 279.

(7) Kranz, M.; Clark, T.; Schleyer, P. v. R. *J. Org. Chem.* **1993**, *58*, 3317.

(8) As must related compounds, [9,10]-dihydrodibenzo[*c*,*g*]phenanthrene isomerizes via the *syn* transition state. This compound does not racemize at 60 °C in benzene. Its half-life in boiling toluene (111 °C) is 218 min. Hall, D. M.; Turner, E. E. *J. Chem. Soc.* **1955**, 1242.

0002-7863/94/1516-4801$04.50/0

= Z' = N; X, X' = Ru(2,2'-bipyridine)$_2$).[9,10] The ligand 1,1'-biisoquinoline is expected to be nonplanar because of unfavorable transannular steric interactions between H_8 and $H_{8'}$. Consequently, **2** is chiral at the metal center and the 1,1'-biisoquinoline ligand and therefore is expected to exist in two diastereomeric forms. Surprisingly, the two diastereomers of **2** are stereochemically labile. We conclude from the present mechanistic study that the interconversion of the two diastereomers of **2** takes place by a regular mechanism (without breaking Ru–N bonds) that involves atropisomerization of the η^2-1,1'-biisoquinoline ligand via a *syn* transition state.

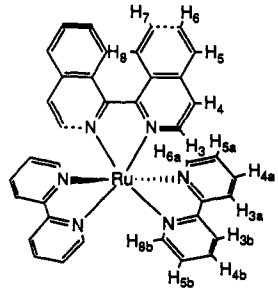

2 = $Ru^{II}(bipy)_2(1,1'\text{-biiq})]^{2+}$

Experimental Section

Materials. $RuCl_3 \cdot nH_2O$ was provided by Johnson-Matthey Co. Ether was distilled from sodium benzophenone diketal. Reagent grade dichloromethane, ethanol, and pentane were used without further purifications. Acetone-d_6, D_2O, and 20% DCl in D_2O were used as received from Aldrich. Lithium diisopropylamide mono(tetrahydrofuran) (LDA) was obtained as a 1.5 M solution in cyclohexane from Aldrich. Hexamethylphosphoramide (HMPA) was vacuum distilled from sodium. Isoquinoline was purified by vacuum distillation from 4-Å molecular sieves. Ru(2,2'-bipyridine)$_2$Cl$_2$[11] and 2,2'-bipyridine-d_8[12] were synthesized according to literature procedures.

Synthesis of 1,1'-Biisoquinoline. Isoquinoline (9.35 g, 72 mmol) and HMPA (12.6 mL, 13.0 g, 72 mmol) were dissolved in dry ether (125 mL) in a nitrogen atmosphere. The resulting solution was cooled to −78 °C (dry ice/acetone bath), and LDA (24.2 mL of 1.5 M cyclohexane solution, 36 mmol) was added dropwise via a Hamilton gas-tight syringe in 10 min. The solution was allowed to stir for 1 h at −78 °C, the bath was removed, and the solution was warmed to room temperature. After being stirred for 1 h at room temperature under an atmosphere of nitrogen, the solution was exposed to air for 12 h. After being quenched with water, the reaction mixture was transferred to a separatory funnel. The ether layer was extracted with water (3 × 100 mL), and the combined aqueous extracts were extracted with ether (3 × 100 mL). The volatiles were removed from the combined ether extracts on a rotary evaporator to give a yellow oil, which was chromatographed on grade I basic alumina, eluting with 95% toluene and 5% methanol. The first band was collected, and the volatiles were removed with a rotary evaporator to give a yellow solid. Recrystallization from benzene/pentane gave 1,1'-biisoquinoline as yellow crystals (5.2 g, 56%). No attempt was made to optimize the reaction conditions. ^{1}H NMR (acetone-d_6, 25 °C, 300 MHz): δ 8.68, 7.96 (d, $H_{3,4}$, J = 5.7 Hz); 8.08 (d, H_5, J = 8.3 Hz); 7.78 (t, H_6); 7.73 (d, H_8, J = 9.4 Hz); 7.54 (t, H_7). Anal. Calcd for $C_{18}H_{12}N_2$: C, 84.35; H, 4.72. Found: C, 84.92; H, 4.43.

Synthesis of (Δ,δ/Λ,λ)-2 (Major) Diastereomer. Ru(2,2'-bipyridine)$_2$Cl$_2$ (125 mg, 0.26 mmol), 1 mL of water, and 3 mL of EtOH were placed into a tube fitted with a high-pressure Teflon stopcock. The solution was freeze–pumped–thawed and left under vacuum. The tube was placed in an 80 °C oil bath for 1 h. After the tube was cooled to room temperature, a N_2 atmosphere was introduced and 1,1'-biisoquinoline (132 mg, 0.52 mmol) was added. The resulting solution was freeze–pumped–thawed, left under vacuum, and returned to the 80 °C oil bath for 6 h. After the tube was cooled to room temperature, the EtOH was removed under vacuum. The remaining solution was filtered through Celite, and the product precipitated upon dropwise addition of aqueous NH_4PF_6 (106 mg, 0.65 mmol in ca. 2 mL of water). The precipitate was removed by filtration, dried under vacuum, and recrystallized by vapor diffusion from CH_2Cl_2/pentane to give large dark-purple crystals (188 mg, 0.20 mmol, 75% based on Ru(bipy)$_2$Cl$_2$). Anal. Calcd for $C_{38}H_{28}F_{12}N_6P_2Ru$: C, 47.56; H, 2.94. Found: C, 47.25; H, 2.87.

Table 1. Crystallographic Data for (Δ,δ/Λ,λ)-**2** at 25 °C[a]

formula	$C_{38}H_{28}F_{12}N_6P_2Ru$
fw	959.68
space group	$C2/c$ (No. 15)
cell dimensions[b]	
a, Å	29.12(1)
b, Å	18.593(7)
c, Å	17.85(1)
β, deg	127.81(4)
V, Å^3	7635(7)
Z	8
d_{calcd}, g cm^{-3}	1.67
crystal shape	rectangular prism
crystal dimensions, mm	0.20 × 0.26 × 0.41
radiation	Mo Kα (λ = 0.710 73 Å)[c]
absorption coefficient, mm^{-1}	0.122
data collection range, deg	3–45
no. of unique data	6733
no. of data used ($I > 2\sigma(I)$)	3614
R	0.053
R_w	0.062
GOF	2.12
largest shift/esd, final cycle	0.21

[a] The standard deviation of the least significant figure is given in parentheses in this and subsequent tables. $R = \sum||F_o| - |F_c||/\sum|F_o|$, $R_w = [\sum\omega(|F_o| - |F_c|)^2/\sum\omega|F_o|^2]^{1/2}$, GOF = $[\sum(\omega(|F_o| - |F_c|)^2/(m-n)]^{1/2}$. [b] The cell dimensions were obtained from a least-squares refinement of the setting angles of 25 reflections. [c] Monochromatized by a graphite crystal.

X-ray Diffraction Study of (Δ,δ/Λ,λ)-2. X-ray data were collected with an Enraf-Nonius CAD4 diffractometer using monochromated Mo Kα radiation (λ = 0.710 69 Å) and methods standard in this laboratory.[13] The crystallographic data are summarized in Table 1. Automatic centering, indexing, and least-squares routines were used to obtain the cell dimensions. The data were collected and corrected for Lorentz and polarization effects;[14] however, no absorption correction was applied since it was judged to be negligible. Crystal integrity was followed by periodically recollecting three reflections. No decay was observed. The structures were solved by direct methods using the SHELX-86[15] program. Refinement of the structures was by full-matrix least-squares calculations using SHELX-76[16] initially with isotropic and finally with anisotropic temperature factors for the non-hydrogen atoms. Neutral scattering factors were used for all atoms.[17] At an intermediate stage of refinement, a difference map revealed maxima consistent with the positions of hydrogen atoms which were included in the subsequent cycles of refinement in idealized positions with isotropic temperature factors that reflected the temperature factors of the aromatic carbon atoms to which they are bound. Unit weights were used in the early stages of refinement, and weights derived from counting statistics were used in the final cycles of refinement. A difference map calculated at the end of the refinement showed no chemically significant features. ORTEP views of (Λ,λ)-**2** are given in Figures 1 and 2. Selected interatomic distances, angles, and torsion angles for (Δ,δ/Λ,λ)-**2** are summarized in Tables 2–4. Listings of the positional and thermal parameters for (Λ,λ)-**2** are included in the supplementary material.

(9) A portion of this work has been reported previously in a preliminary communication: Ashby, M. T.; Govindan, G. N.; Grafton, A. K. *Inorg. Chem.* **1993**, *32*, 3803.

(10) Compound **2** completes the series [Ru(2,2'-bipyridine)$_2$(LL)]$^{2+}$, where LL are symmetric benzannelated bipyridine ligands, i.e., 1,1'-biisoquinoline, 3,3'-biisoquinoline (Juris, A.; Barigelletti, F.; Balzani, V.; Belser, P.; Zelewsky, A. *Inorg. Chem.* **1985**, *24*, 202), and 2,2'-biquinoline (Belser, P.; von Zelewsky, A. *Helv. Chim. Acta* **1980**, *63*, 1675).

(11) Sullivan, B. P.; Salmon, D. J.; Meyer, T. J. *Inorg. Chem.* **1978**, *17*, 3334.

(12) Chirayil, S.; Thummel, R. P. *Inorg. Chem.* **1989**, *28*, 812.

(13) (a) Khan, M. A.; Taylor, R. W.; Lehn, J. M.; Dietrich, B. *Acta Crystallogr.* **1988**, *C44*, 1928. (b) Ashby, M. T.; Khan, M. A.; Halpern, J. *Organometallics* **1991**, *10*, 2011.

(14) Walker, N.; Stuart, D. *Acta Crystallogr.* **1983**, *A39*, 158.

(15) Sheldrick, G. M. In *Crystallographic Computing 3*; Sheldrick, G. M., Kruger, C., Goddard, R., Eds.; Oxford University Press: Oxford, England, 1985; pp 175–189.

(16) Sheldrick, G. M. *SHELX-76. A Program for Crystal Structure Determination*; University of Cambridge: Cambridge, England, 1976.

(17) *International Tables for X-ray Crystallography*; Kynoch Press: Birmingham, England, 1974; Vol. IV, pp 99, 149.

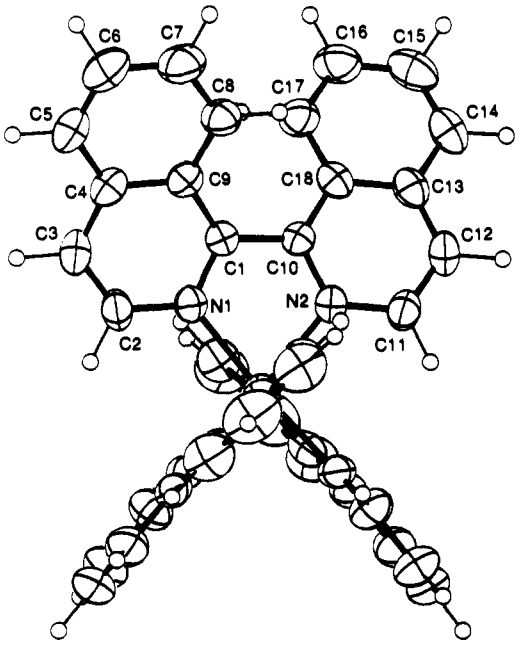

Figure 1. ORTEP drawing of (Λ,λ)-**2** showing the labeling scheme of the 1,1′-biisoquinoline ligand. Atoms are represented by thermal vibration ellipsoids at the 50% level. Hydrogen atoms have been assigned arbitrary thermal parameters.

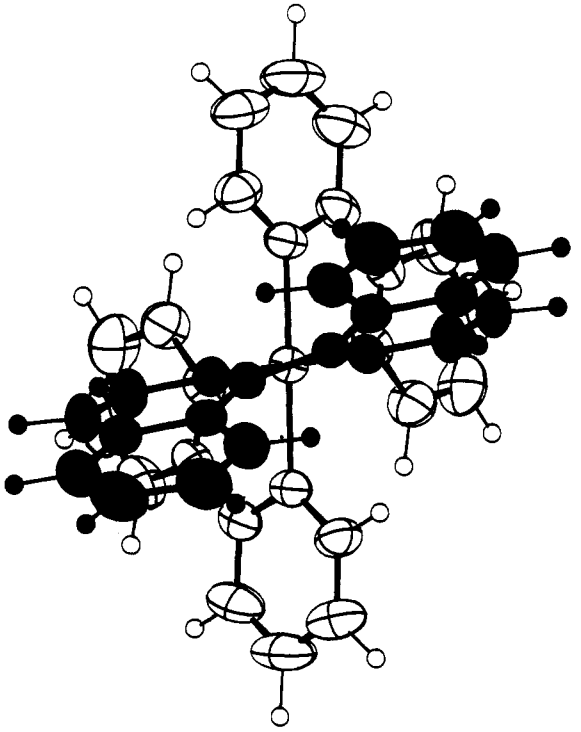

Figure 2. Top-down ORTEP drawing of (Λ,λ)-**2** showing the nonplanarity of the 1,1′-biisoquinoline ligand. Atoms are represented by thermal vibration ellipsoids at the 50% level. Hydrogen atoms have been assigned arbitrary thermal parameters. The 1,1′-biisoquinoline ligand is shaded.

NMR Sample Preparation. Single crystals of compound **2** were dissolved in the deuterated solvent (acetone-d_6 or D_2O) to give 10–20 mM solutions. The solutions were transferred to 5-mm NMR tubes that had been glass blown onto vacuum line adaptors fitted with high-vacuum Teflon stopcocks. The samples were put through two freeze–pump–thaw cycles and left under vacuum, and then the tubes were flame-sealed while the solutions were frozen.

Assignment of ^{1}H NMR Spectrum of 2. Scalar coupling relationships between the protons were obtained using ^{1}H–^{1}H double-quantum-filtered homonuclear correlation spectroscopy (dqf-COSY)[18] at −80 °C, conditions under which chemical exchange is slow. Assignments are based upon the assumption that most of the corresponding resonances of the 2,2′-bipyridine ligands of each diastereomer exhibit nearly the same chemical shifts. The one exception is H_{6a} (data shown bold below), which is significantly shielded[19] by the aromatic ring of the 1,1′-biisoquinoline ligand in the minor isomer. (Δ,δ/Λ,λ)-**2** (major) diastereomer, ^{1}H NMR (acetone-d_6, 25 °C, 500 MHz): δ 8.85 (d, bipy-H_{3b}, J = 8.0 Hz); 8.79 (d, bipy-H_{3a}, J = 8.0 Hz); **8.65 (d, bipy-H_{6a}, J = 7.0 Hz)**; 8.25 (dt, bipy-H_{4b}, J = 7.0, 8.0 Hz); 8.18 (d, biiq-H_5, J = 8.0 Hz); 8.17 (d, biiq-H_8, J = 8.0 Hz); 8.12 (dt, bipy-H_{4a}, J = 7.0, 8.0 Hz); 8.03 (s, biiq-$H_{3,4}$); 8.02 (t, bipy-H_{6b}, J = 7.0 Hz); 7.93 (t, biiq-H_7, J = 8.0 Hz); 7.75 (t, biiq-H_6, J = 8.0 Hz); 7.61 (dt, bipy-H_{5b}, J = 7.0, 8.0 Hz); 7.40 (dt, bipy-H_{5a}, J = 7.0, 8.0 Hz). (Δ,λ/Λ,δ)-**2** (minor) diastereomer, ^{1}H NMR (acetone-d_6, 25 °C, 500 MHz): δ 8.87 (d, bipy-H_{3b}, J = 8.0 Hz); 8.79 (d, bipy-H_{3a}, J = 8.0 Hz); 8.41 (d, biiq-H_8, J = 8.0 Hz); 8.25 (dt, bipy-H_{4b}, J = 7.0, 8.0 Hz); 8.24, 8.09 (d, biiq-$H_{3,4}$, J = 7.0 Hz); 8.17 (d, biiq-H_5, J = 8.0 Hz); 8.13 (dt, bipy-H_{4a}, J = 7.0, 8.0 Hz); 8.10 (t, bipy-H_{6b}, J = 7.0 Hz); 8.01 (t, biiq-H_6, J = 8.0 Hz); 7.80 (t, biiq-H_7, J = 8.0 Hz); 7.62 (dt, bipy-H_{5b}, J = 7.0, 8.0 Hz); 7.39 (dt, bipy-H_{5a}, J = 7.0, 8.0 Hz); **7.05 (d, bipy-H_{6a}, J = 7.0)**. The chemical shifts in D_2O solvent are comparable.

Spin Saturation Transfer (SST) Studies (Multiplicity of Exchange). SST rate data were obtained using standard procedures,[20] and the rate constants were determined by least-squares fits of the first-order data. The rates that were measured using the SST method agreed well with those independently measured using the SIT method: e.g., $k(6a_{maj}\rightarrow 6a_{min})$ = 12.3(9) s^{-1} and $k(6a_{min}\rightarrow 6a_{maj})$ = 37(2) s^{-1} at 80 °C. The kinetic data that were obtained from the SST experiments are summarized in Table 5 (top).

Table 2. Selected Interatomic Distances for (Λ,λ)-**2** (Å)

atoms	distance	atoms	distance	atoms	distances
Ru–N1	2.061(4)	N4–C25	1.344(7)	C7–C8	1.355(8)
Ru–N2	2.062(4)	N5–C29	1.353(6)	C8–C9	1.423(8)
Ru–N3	2.053(4)	N5–C30	1.348(8)	C10–C18	1.432(7)
Ru–N4	2.063(4)	N6–C34	1.360(7)	C11–C12	1.348(8)
Ru–N5	2.070(4)	N6–C35	1.342(8)	C12–C13	1.399(8)
Ru–N6	2.048(4)	C1–C9	1.427(7)	C13–C14	1.422(8)
N1–C1	1.347(6)	C1–C10	1.478(8)	C13–C18	1.425(9)
N1–C2	1.374(9)	C2–C3	1.352(8)	C14–C15	1.348(10)
N2–C10	1.350(6)	C3–C4	1.401(8)	C15–C16	1.398(12)
N2–C11	1.373(9)	C4–C5	1.421(8)	C16–C17	1.358(8)
N3–C19	1.372(7)	C4–C9	1.424(9)	C17–C18	1.421(8)
N3–C20	1.338(8)	C5–C6	1.347(9)		
N4–C24	1.361(6)	C6–C7	1.401(11)		

Table 3. Selected Interatomic Angles for (Λ,λ)-**2** (deg)[a]

atoms	angle	atoms	angle
N1–Ru–N2	77.90(18)	Ru–N1–C1	115.7(4)
N1–Ru–N3	97.41(17)	Ru–N1–C2	124.4(3)
N1–Ru–N4	174.74(16)	Ru–N2–C10	115.6(4)
N1–Ru–N5	97.80(18)	Ru–N2–C11	124.7(3)
N1–Ru–N6	88.77(16)	Ru–N3–C19	114.6(4)
N2–Ru–N3	88.44(16)	Ru–N3–C20	125.8(4)
N2–Ru–N4	97.80(18)	Ru–N4–C24	114.9(4)
N2–Ru–N5	174.81(15)	Ru–N4–C25	126.4(4)
N2–Ru–N6	97.67(16)	Ru–N5–C29	114.9(4)
N3–Ru–N4	79.32(7)	Ru–N5–C30	125.9(4)
N3–Ru–N5	95.05(17)	Ru–N6–C34	115.1(4)
N3–Ru–N6	172.12(15)	Ru–N6–C35	125.8(4)
N4–Ru–N5	86.65(17)	L1–Ru–L2	121.11(3)
N4–Ru–N6	94.86(17)	L2–Ru–L3	117.51(1)
N5–Ru–N6	79.21(17)	L1–Ru–L3	121.37(3)

[a] L1 is the midpoint of the σ-bond of the 1,1′-biisoquinoline ligand. L2 and L3 are the midpoints of the σ-bonds of the 2,2′-bipyridine ligands.

Table 4. Selected Torsion Angles for (Λ,λ)-**2** (deg)

atoms	angle
N1–C1–C10–N2	−24.1(6)
N3–C19–C24–N4	−3.4(8)
N5–C29–C34–N6	−3.0(8)

(18) Rance, M.; Sorensen, O. W.; Bodenhausen, G.; Wagner, G.; Ernst, R. R.; Wüthrich, K. *Biochem. Biophys. Res. Commun.* **1983**, *117*, 479.
(19) Johnson, C. E., Jr.; Bovey, F. A. *J. Chem. Phys.* **1958**, *29*, 1021.
(20) (a) Faller, J. W. *Adv. Organomet. Chem.* **1977**, *16*, 211. (b) Green, M. L. H.; Sella, A.; Wong, L.-L. *Organometallics* **1992**, *11*, 2650.

Table 5. Kinetic and Thermodynamic Data[a]

resonance irradiated	resonance exchanging	k (s^{-1})	K	solvent	T (°C)
Spin Saturation Transfer (SST) Experiments					
bipy-H_{6a} (maj)	bipy-H_{6a} (min)	12.3(9)	2.89	acetone-d_6	80
bipy-H_{6a} (min)	bipy-H_{6a} (maj)	37(2)	2.89	acetone-d_6	80
bipy-H_{6b} (maj)	bipy-H_{6a} (maj)	~0	2.89	acetone-d_6	80
bipy-H_{6b} (maj)	bipy-H_6 (min)	~0	2.89	acetone-d_6	80
bipy-H_{6b} (min)	bipy-H_{6a} (maj)	~0	2.89	acetone-d_6	80
bipy-H_{6b} (min)	bipy-H_{6a} (min)	~0	2.89	acetone-d_6	80
Spin Inversion Transfer (SIT) Experiments					
biiq-H_3 (maj)	biiq-H_3 (min)	12.8(8)	2.89	acetone-d_6	80
bipy-H_{6a} (maj)	bipy-H_{6a} (min)	1.43(6)	2.71	acetone-d_6	50
bipy-H_{6a} (maj)	bipy-H_{6a} (min)	3.3(1)	2.76	acetone-d_6	60
bipy-H_{6a} (maj)	bipy-H_{6a} (min)	6.9(2)	2.86	acetone-d_6	70
bipy-H_{6a} (maj)	bipy-H_{6a} (min)	12.7(3)	2.88	acetone-d_6	80
bipy-H_{6a} (maj)	bipy-H_{6a} (min)	27(2)	3.04	acetone-d_6	90
bipy-H_{6a} (min)	bipy-H_{6a} (maj)	36.6(9)	2.89	acetone-d_6	80
bipy-H_{6a} (maj)	bipy-H_{6a} (min)	5.7(2)	2.63	1 M LiCl in D_2O[b]	80
bipy-H_{6a} (maj)	bipy-H_{6a} (min)	7.1(1)	2.63	1 M DCl in D_2O[b]	80

[a] $[Ru^{II}(bipy)_2(1,1'\text{-biiq})](PF_6)_2$ was used for the experiments in acetone in which bipy rate constants were measured. $[Ru^{II}(bipy\text{-}d_8)_2(1,1'\text{-biiq})](PF_6)_2$ was used for the experiment in acetone in which the biiq rate constant was measured. $[Ru^{II}(bipy)_2(1,1'\text{-biiq})](Cl)_2$ was used for the experiments in water. The activation parameters calculated from the rate date at 50–90 °C are $\Delta H^{\ddagger}$(maj→min) = 68.7 kJ mol^{-1}, $\Delta S^{\ddagger}$(maj→min) = –21 J K^{-1} mol^{-1}, $\Delta H^{\ddagger}$(min→maj) = 66.1 kJ mol^{-1}, and $\Delta S^{\ddagger}$(min→maj) = –38 J K^{-1} mol^{-1}. [b] The concentration of **2** was 15 mM.

Spin Inversion Transfer (SIT) Studies (Rates of Exchange). SIT rate data were obtained using the standard pulse sequence: d_1, $\pi/2$, d_2, $\pi/2$, τ_m, $\pi/2$, aq.[21] The transmitter offset frequency was set equal to ν_A, the frequency of the nucleus to be inverted. The relaxation delay d_1 was set equal to 5 times the longest T_1 to allow complete longitudinal relaxation between pulses. The second delay was set equal to $1/(2|\nu_A - \nu_B|)$, where $|\nu_A - \nu_B|$ is the frequency difference between the nucleus to be inverted and the exchanging nucleus. The mixing time τ_m was typically varied from 0.001 s to about $5T_1$. The 90° pulse width was determined experimentally prior to each kinetics run. The rate constants and T_1 relaxation times were obtained by nonlinear least-squares fits of the equations that describe the recovery of the inverted resonance (A) and the effect on the resonance that corresponds to the hydrogen atom(s) undergoing chemical exchange (B):

$$A \underset{k_b}{\overset{k_a}{\rightleftharpoons}} B$$

$$M_z^A(t) = c_1 \exp(\lambda_1 t) + c_2 \exp(\lambda_2 t) + M_\infty^B \quad (1)$$

$$M_z^B(t) = (c_1/k_a)(\lambda_1 + k_b^{eff}) \exp(\lambda_1 t) + (c_2/k_a)(\lambda_2 + k_b^{eff}) \exp(\lambda_2 t) + M_\infty^A \quad (2)$$

where c_1, c_2, λ_1, and λ_2 are constants defined by

$$\lambda_1 = \{-(k_a^{eff} + k_b^{eff}) + [(k_a^{eff} + k_b^{eff})^2 - 4((k_a^{eff}k_b^{eff}) - (k_a k_b))]^{1/2}\}/2 \quad (3)$$

$$\lambda_2 = \{-(k_a^{eff} + k_b^{eff}) - [(k_a^{eff} + k_b^{eff})^2 - 4((k_a^{eff}k_b^{eff}) - (k_a k_b))]^{1/2}\}/2 \quad (4)$$

$$c_1 = M_0^B - M_\infty^B - c_2 \quad (5)$$

$$c_2 = (k_a/(\lambda_1 - \lambda_2))\,(\lambda_1 + k_b^{eff})(M_0^B - M_\infty^B)/k_a + M_\infty^A - M_0^A \quad (6)$$

The effective first-order rate constants are represented as the sums of the two first-order rate constants for the pathways that lead to a loss of magnetization, chemical exchange and spin–lattice relaxation:

$$k_a^{eff} = k_a + 1/T_{1a} \quad (7)$$

(21) (a) Alger, J. R.; Prestegard, J. H. *J. Magn. Reson.* **1977**, *27*, 137. (b) Kuchel, R. W.; Chapman, B. E. *J. Theor. Biol.* **1983**, *105*, 569. (c) Robinson, G.; Kuchel, P. W.; Chapman, B. E. *J. Magn. Reson.* **1985**, *63*, 314. (d) Bellon, S. F.; Chen, D.; Johnston, E. R. *J. Magn. Reson.* **1987**, *73*, 168.

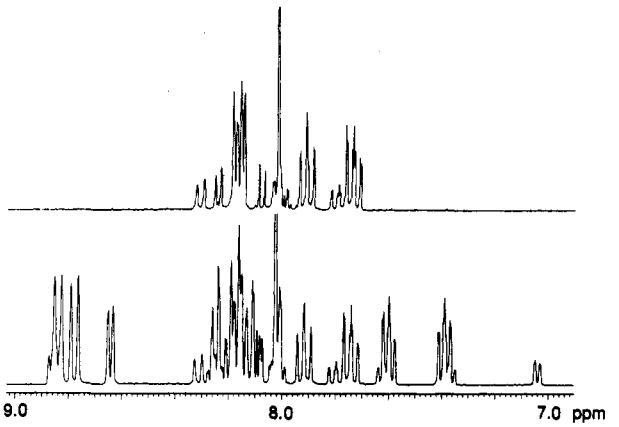

Figure 3. ^1H NMR spectra of **2** and **2**-d_{16} at 300 MHz and 25 °C.

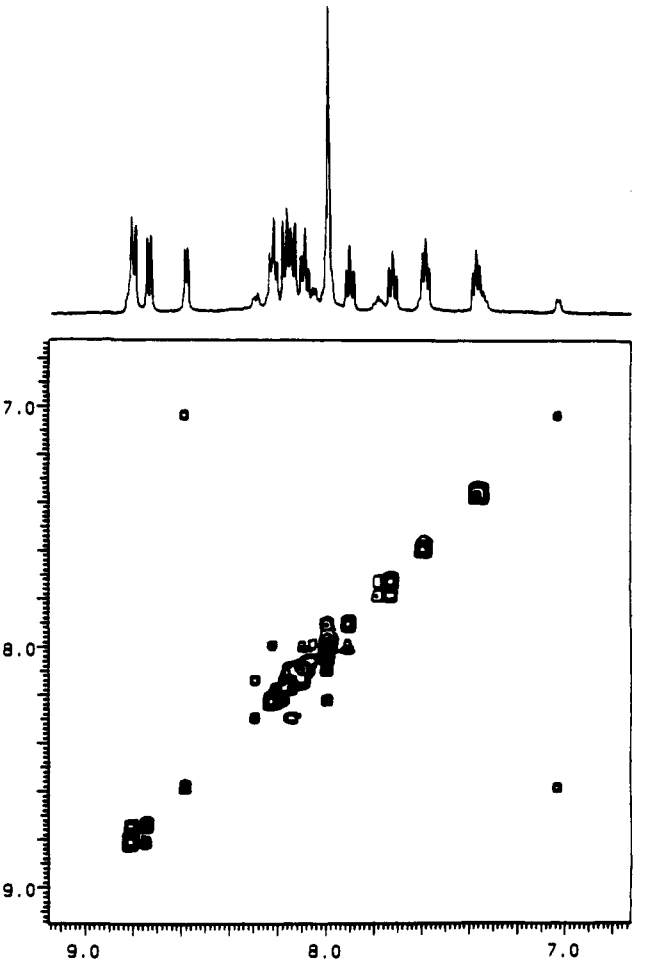

Figure 4. 2D EXSY spectrum at 500 MHz and 80 °C revealing the interconversion of (Δ,δ/Λ,λ)-**2** and (Δ,λ/Λ,δ)-**2**.

$$k_b^{eff} = k_b + 1/T_{1b} \quad (8)$$

The data consisting of peak amplitude versus delay time τ_m were analyzed by fitting eqs 1 and 2 to the experimental data. The analysis was performed on a Silicon Graphics IRIS Indigo XS24 running the nonlinear least-squares regression program SPIRAL.[22] The nonlinear regression yielded values and estimated errors for k_a, M_0^A, M_0^B, T_{1a}, and T_{1b}. The reverse rate constants k_b were calculated from the equilibrium concentrations:

$$k_b = k_a/K \quad (9)$$

Typical fits for spin transfer and inversion recovery are illustrated in Figure 5. The kinetic data that were obtained from the SIT experiments are summarized in Table 5 (bottom).

(22) Jones, A. *J. Comput. Phys.* **1970**, *13*, 201.

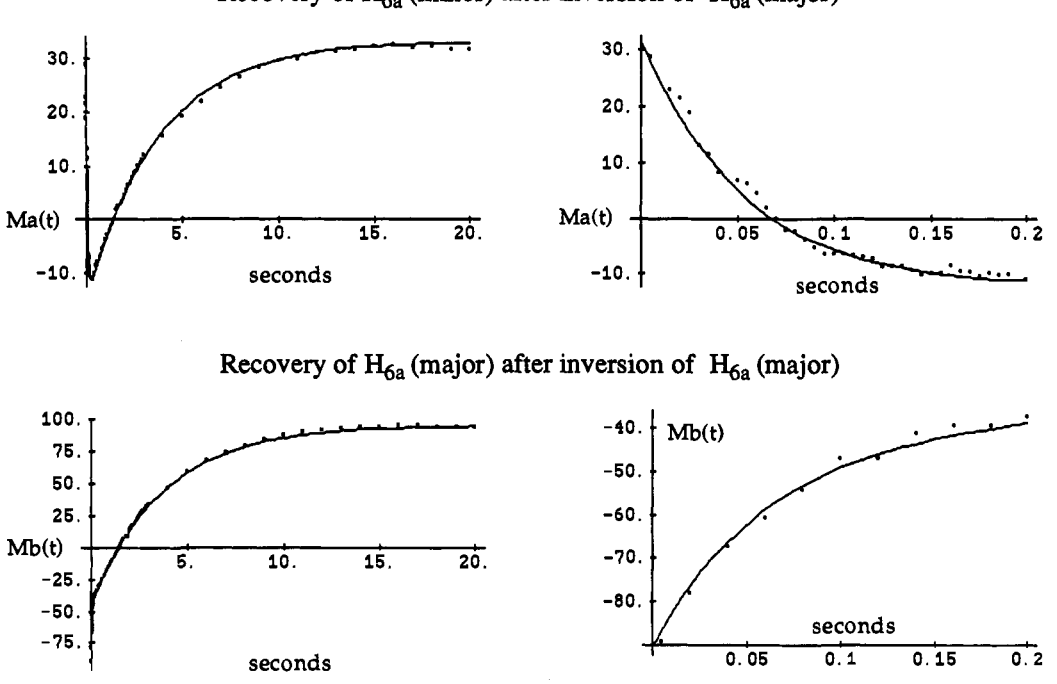

Figure 5. Nonlinear least-squares fit of the spin inversion transfer data used to calculate $k(6a_{maj} \rightarrow 6a_{min})$. The ordinate is an arbitrary scale. Note that the half-life for chemical exchange of H_{6a}(minor) with H_{6a}(major) is $\tau_{min} = 0.027$ s, whereas the spin–lattice relaxation time for H_{6a}(minor) and H_{6a}(major) is $T_1 \approx 4$ s.

2D EXSY Studies (Symmetry of Exchange). The two-dimensional exchange spectroscopy (2D EXSY) pulse sequence is essentially the same as that used for nuclear Overhauser effect spectroscopy (NOESY): d_1, $\pi/2$, d_2, $\pi/2$, τ_m, $\pi/2$, aq.[23] The relaxation delay d_1 was set equal to 5 times the longest T_1 to allow complete longitudinal relaxation between pulses. Because of the long d_1 delay time, a homospoil–$\pi/2$–homospoil presequence was unnecessary. A mixing time of $\tau_m = 0.1$ s was used to obtain the spectrum of Figure 4 at 80 °C; however, varying τ_m had no effect on the qualitative features of the spectrum. The spectrum illustrates only the positive peaks; therefore, the cross peaks corresponding to chemical exchange are observed. Weak negative cross peaks that correspond to NOE coupling were also observed. Increasing the threshold of the spectrum of Figure 4 reveals positive cross peaks that result from zero-quantum coherence (zero-quantum-filtered COSY), but the latter peaks are substantially weaker than the cross peaks that are attributed to chemical exchange.

Results

Assignment of the Specific Relative Configuration of 2 in Solution. The ^{1}H NMR spectrum of **2** reveals an ~3:1 mixture of the two diastereomers in acetone solutions at 25 °C. A single-crystal X-ray structure determination of **2** was undertaken to obtain more information regarding its structure. Surprisingly, only one of the two diastereomers was found to crystallize from acetonitrile/ether (quantitative yield based on total Ru). The latter result implies that the two diastereomers of **2** are in equilibrium on the time scale of the crystallization (1 week). Compound **2** crystallizes in a centrosymmetric space group as pairs of enantiomers; the conformation of the five-membered chelate ring is λ when the configuration at the metal is Λ (Figures 1 and 2). Remarkably, the ^{1}H NMR spectrum obtained a few minutes after the single crystal used in the X-ray study was dissolved in acetone at 25 °C again revealed an ~3:1 mixture of the diastereomers (Figure 3). A second single crystal, which proved to have the same cell dimensions as the crystal used in the X-ray study, was dissolved in acetone at −80 °C; the resulting ^{1}H NMR spectrum was that of the major diastereomer. After the sample was warmed to 25 °C, an ~3:1 ratio of the two diastereomers of **2** was again observed. The ~3:1 ratio was maintained when the same sample was cooled again to −80 °C. Thus the structure of **2** found in the solid state (δ/Δ,λ/Λ) is that of the major diastereomer in solution.

Assignment of the ^{1}H NMR Spectrum of 2. We have investigated the fluxional behavior of **2** using dynamic nuclear magnetic resonance (DNMR) spectroscopy. The use of such methods to follow the dynamics of isomerization of labile metal complexes is generally hampered by the need to unambiguously assign the NMR spectrum. There are a total of 28 magnetically inequivalent nuclei between the two diastereomers of **2**. The ^{1}H NMR spectra of each diastereomer of **2** are particularly complicated because they consists of three four-spin ABCD systems of equal weight. We synthesized the derivative of **2** containing 2,2'-bipyridine-d_8 ligands[12] in order to differentiate between the ABCD resonances associated with the 1,1'-biisoquinoline ligand and those of the unsymmetic 2,2'-bipyridine ligands. The ^{1}H NMR spectrum of **2**-d_{16} is shown in Figure 3. The ^{1}H NMR spectrum of **2**-d_{16} is identical to the protio derivative in the 1,1'-biisoquinoline regions; no significant isotope shifts are observed. An added benefit of **2**-d_{16} is that most of the overlapping resonances of the major diastereomer were eliminated, which further simplified the DNMR studies (*vide infra*).

Coupling relationships between the protons were determined using ^{1}H–^{1}H double-quantum-filtered homonuclear correlation spectroscopy (dqf-COSY) at −80 °C, conditions under which chemical exchange is slow with respect to spin relaxation. Assignments are based upon the assumption that most of the resonances that correspond to the 2,2'-bipyridine ligands in the two diastereomers exhibit nearly the same chemical shifts. The one exception is H_{6a}, which is significantly shielded by the aromatic ring of the 1,1'-biisoquinoline ligand in the minor isomer. The latter observation is an important one, for it differentiates between the two inequivalent pyridine groups of the 2,2'-bipyridine ligands, which will prove important in distinguishing between alternative mechanisms (*vide infra*).

Although not essential to the conclusions of the paper, the results of the X-ray analysis of (Δ,δ/Λ,λ)-**2** have enabled us to assign the ^{1}H NMR spectra of the diastereomers of **2**. The

(23) Abel, E. W.; Coston, T. P. J.; Orrell, K. G.; Sik, V.; Stephenson, D. *J. Magn. Reson.* **1986**, *70*, 34.

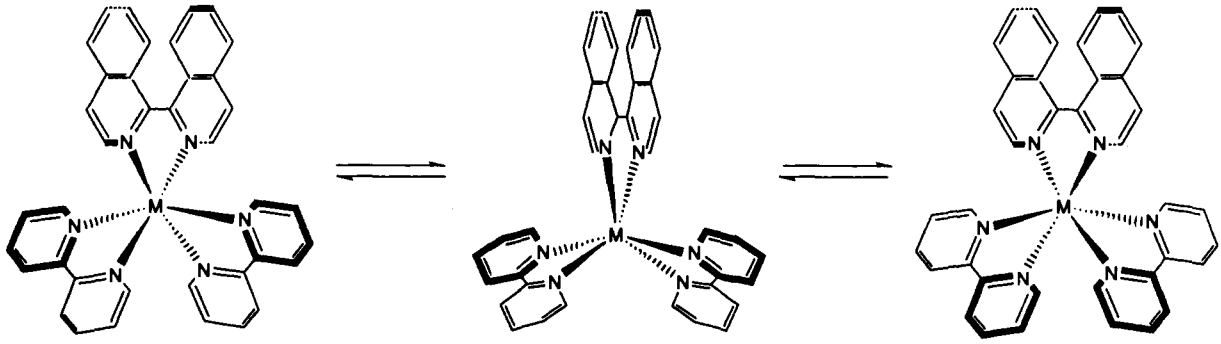

Figure 6. Bailar twist mechanism. Note that the C_2 symmetry of the molecule is preserved during the isomerization reaction but the *cis*/*trans* relationship of the 2,2′-bipyridine ligands is not. The pyridyl groups that are *cis* (with respect to the 1,1′-biisoquinoline ligand) in the diastereomer on the left (bold rings) become *trans* in the diastereomer on the right (and vice versa).

shielding effects of the isoquinoline groups on H_{6a} are also consistent with the assignment of the stereochemistry. Thus the isoquinoline ring is situated over H_{6a} in the minor isomer and is rotated away in the major isomer. Besides explaining the ^1H NMR spectra, this contact may also explain the reason behind the fact that the major isomer is thermodynamically favored; an analysis of the two geometries with molecular mechanics calculations shows that the only significant difference between the two diastereomers is the latter contact.

Molecularity of Exchange. Interconversion of (Δ,δ/Λ,λ)-**2** and (Δ,λ/Λ,δ)-**2** is not taking place via complete dissociation of the 1,1′-biisoquinoline ligand since we do not observe the capture of $[Ru^{II}(2,2'\text{-bipyridine})_2]^{2+}$ by added 2,2′-bipyridine to give the inert $[Ru^{II}(2,2'\text{-bipyridine})_3]^{2+}$ and since spin-labeled free 1,1′-biisoquinoline and 2,2′-bipyridine do not exchange with **2** on the time scale of isomerization. The 2D EXSY spectrum of a solution of 1,1′-biisoquinoline and **2** (~3:1) shows no cross peaks corresponding to exchange of free and coordinated 1,1′-biisoquinoline. The interconversion is therefore intramolecular.

Symmetry of Exchange. Because chemical exchange is slow on the NMR time scale, a discrete, static spectrum is obtained for the two diastereomers of **2**. However, as it turns out, chemical exchange is fast with respect to spin–lattice relaxation. Accordingly, spin perturbation/recovery techniques may used to probe the kinetics of isomerization; the three NMR methods that are generally employed are spin saturation transfer (SST),[20] spin inversion transfer (SIT),[21] and two-dimensional exchange spectroscopy (2D EXSY).[23] We employed 2D EXSY to investigate the symmetry of chemical exchange. A complete assignment of the ^1H NMR spectra of **2** is necessary to interpret the results of the 2D EXSY experiment. In particular, it is necessary to assign the resonances that correspond to the symmetry-inequivalent halves of the 2,2′-bipyridine ligands. Fortunately, this proved possible for **2** (*vide supra*). The 2D EXSY spectrum of **2** is illustrated in Figure 4. Note in particular the cross peak that corresponds to chemical exchange between H_{6a}(major) at 8.65 ppm and H_{6a}(minor) at 7.05 ppm. Since no cross peaks are observed that correspond to chemical exchange of H_{6a}(major) with H_{6b}(minor) or of H_{6b}(major) with H_{6a}(minor), it is clear that the C_2 symmetry and *cis*/*trans* relationship of the 2,2′-bipyridine ligands are maintained during the interconversion of the diastereomers.

Kinetics of Exchange. Complete assignment of the ^1H NMR spectra of **2** is in fact unnecessary for the kinetic studies. It is only necessary to unambiguously identify one resonance for the 1,1′-biisoquinoline and one resonance for each inequivalent pyridine group of the unsymmetrical 2,2′-bipyridine ligands. The two spin perturbation methods that are generally employed to measure the kinetics of chemical exchange are SST and SIT. Each method has its advantages and disadvantages. SST may be applied to multisite exchange problems, but SIT works only with two-site exchange problems. Since the 2D EXSY spectrum indicates that we are dealing with a two-site exchange problem, either method will work. SIT data are generally more accurate than SST data. However, both the resonance that is spin-perturbed and the resonance that is undergoing chemical exchange must be integrated in the SIT experiment, whereas only the resonance corresponding to the nucleus that is undergoing chemical exchange with the saturated nucleus need be integrated in the SST experiment. Unfortunately, many of the resonances of interest overlap with one another in the ^1H spectrum of **2**. It was possible to measure the kinetics of chemical exchange of the 2,2′-bipyridine groups using the SST method; however, due to unfavorable overlap between the 1,1′-biisoquinoline ligand and the 2,2′-bipyridine ligand, it was not possible to measure the kinetics of exchange of the 1,1′-biisoquinoline ligand. The pseudo-first-order rate constants measured using the SST method are $k(6a_{maj} \rightarrow 6a_{min}) = 12.3(9)\ s^{-1}$ and $k(6a_{min} \rightarrow 6a_{maj}) = 37(2)\ s^{-1}$ at 80 °C. We determined the rate of exchange of the "b" ring of the major diastereomer and the "a" ring of the minor diastereomer to be ca. zero: $k(6b_{maj} \rightarrow 6a_{min}) \approx 0\ s^{-1}$ and $k(6b_{min} \rightarrow 6a_{maj}) \approx 0\ s^{-1}$ at 80 °C. However, a small amount of equilibrium saturation transfer (~10%) was observed upon prolonged irradiation of the sample. A disadvantage of the SST method is that the sample is irradiated for varied periods of time through the decoupler channel. If the decoupler is not selective, partial saturation of adjacent nuclei is possible. This can lead to complicated relaxation kinetics. We believe the latter "leakage" accounts for the small amount of equilibrium saturation transfer that is observed.

The spin perturbation pulse sequence is always the same in the SIT experiment; only the evolution time is varied to allow time for chemical exchange. The SIT method is therefore preferred when the spin-perturbed nucleus and the nucleus that is undergoing chemical exchange exhibit similar chemical shifts and selective spin saturation is not possible. Furthermore, the SIT method is more sensitive than the SST method. Because the resonances that correspond to H_{6a}(major) and H_{6a}(minor) are isolated, we were able to use the protio derivative of **2** to measure the rate of exchange between the "a" rings of the 2,2′-bipyridine ligands of the major and minor diastereomers using the SIT method: $k(6a_{maj} \rightarrow 6a_{min}) = 12.7(3)\ s^{-1}$ (Figure 5). However, it was necessary to use **2**-d_{16}, which is much less congested in the 1,1′-biisoquinoline region, to measure the rate of exchange of the 1,1′-biisoquinoline ligands of the major and minor isomers: $k(3_{maj} \rightarrow 3_{min}) = 12.8(8)\ s^{-1}$. As expected given the symmetry of the exchange process determined by the 2D EXSY experiment, the rates of exchange of the 1,1′-biisoquinoline and 2,2′-bipyridine rings are the same. It is important to reiterate that had this been a multisite exchange problem, the SIT method would not have worked.

Discussion

Following the axiom that mechanisms cannot be proven but that alternative mechanisms can be disproven, we will first discuss

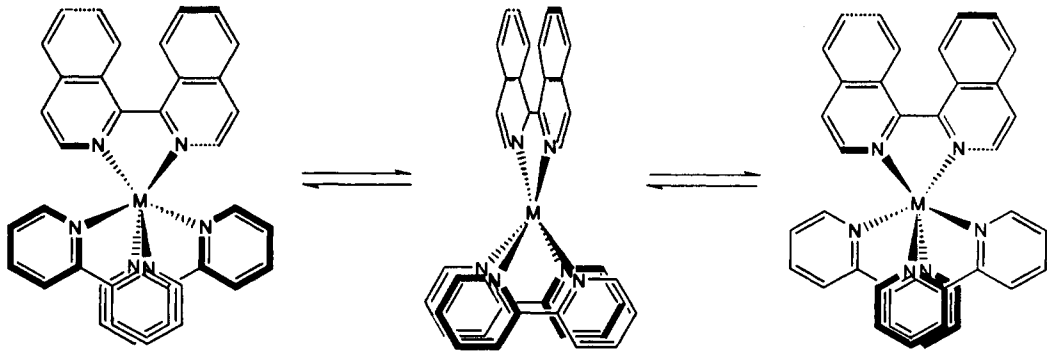

Figure 7. Rây–Dutt twist mechanism. Note that the C_2 symmetry of the molecule is preserved during the isomerization reaction but the *cis/trans* relationship of the 2,2′-bipyridine ligands is not. The pyridyl groups that are *cis* (with respect to the 1,1′-biisoquinoline ligand) in the diastereomer on the left (bold rings) become *trans* in the diastereomer on the right (and vice versa).

the mechanisms that are inconsistent with the experimental data that we have amassed. This discussion will lead to only one credible mechanism. Several mechanisms can be ruled out on symmetry grounds. The SIT and EXSY experiments demonstrate that the C_2 symmetry of **2** and the *cis/trans* relationship of the 2,2′-bipyridine ligands are maintained during the interconversion of the diastereomers (Figures 4 and 5). These experiments eliminate regular mechanisms that involve twisting the ligands in a way that preserves the C_2 axial symmetry of the molecule but interchange the *cis/trans* relationship of the 2,2′-bipyridine ligands with respect to the 1,1′-biisoquinoline ligand. The Bailar twist (Figure 6) and Rây–Dutt twist (Figure 7) are examples of such mechanisms. Also, interconversion of the diastereomers of **2** through an irregular mechanism that involves dissociation of one of the isoquinoline donors of 1,1′-biisoquinoline to give a five-coordinate intermediate that subsequently rotates one or both of the bidentate ligands in a way that destroys the C_2 relationship between the ligands (e.g., productive Berry and some turnstile pseudorotations) is not possible (Figure 8).

Having ruled out the conventional mechanisms for isomerization at the metal center, we considered three alternative mechanisms. There are two plausible mechanisms that involve dissociation of one end of the 1,1′-biisoquinoline that are consistent with the kinetic data that have been discussed thus far: (1) ~360° rotation about the σ-bond of the η^1-1,1′-biisoquinoline ligand or (2) turnstile rotation of the five-coordinate metal center in a way that preserves the C_2 symmetry and *cis/trans* relationship of the 2,2′-bipyridine ligands (Figures 9 and 10). A third regular mechanism, one that does not involve bond breaking, has also thus far not been ruled out: (3) isomerization of the ligand via a planar η^2-1,1′-biisoquinoline (Figure 11). At first glance, none of these three mechanisms appears particularly attractive. The first mechanism, rotation about the σ-bond of an η^1-1,1′-biisoquinoline ligand, would require a rotational barrier lower than that of 1,1′-binaphthyl; atropisomerization of 1,1′-binaphthyl involves bringing H_2 and $H_{8'}$ in close proximity and has a half-life of ~10 h at 25 °C in several solvents.[3] Since the Ru(2,2′-bipyridine)$_2$ moiety is substantially larger than the hydrogen atom substituent in the C_2 position of 1,1′-binaphthyl, one might expect the barrier to rotation about the σ-bond of the intermediate [Ru^{II}(2,2′-bipyridine)$_2$(η^1-1,1′-biisoquinoline)]$^{2+}$ to be greater than that observed for 1,1′-binaphthyl. In fact, the rotational barrier for 1,1′-binaphthyl is 23.5 kcal mol^{-1},[3a] about 7–8 kcal mol^{-1} higher in energy than the barrier observed for interconverting the two diastereomers of **2** (15.8 kcal mol^{-1} for min→maj and 16.4 kcal mol^{-1} for maj→min). The second mechanism, a turnstile rotation, would involve the uncommon pentagonal-planar geometry.[24] Models suggest such a geometry would be seriously sterically encumbered. The third mechanism, rotation about the σ-bond of an η^2-1,1′-biisoquinoline ligand, also requires a rotational barrier lower than those of model compounds. For example, the rotational barrier about the 1,1′ σ-bond of 9,10-dihydrophenanthrene is 28.4 kcal mol^{-1} (a barrier of 27.2 kcal mol^{-1} has been calculated for atropisomerization of 1,1′-binaphthyl via the *syn* transition state),[7,8] which is about 10 kcal mol^{-1} higher in energy than the barrier we have determined for **2**.

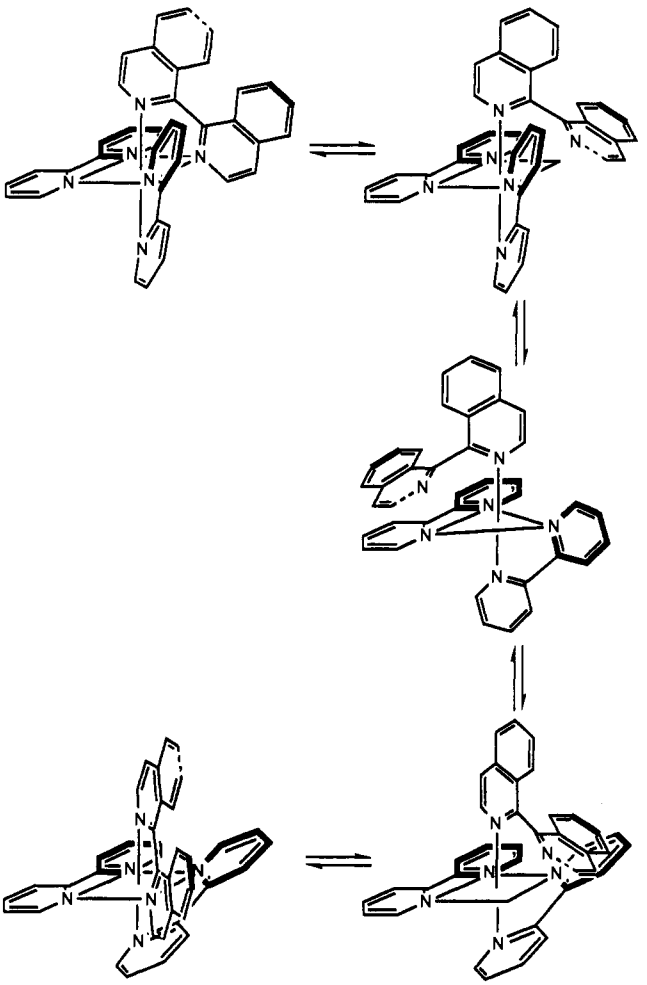

Figure 8. Berry pseudorotation mechanism. Note that neither the C_2 symmetry of the molecule nor the *cis/trans* relationship of the 2,2′-bipyridine ligands is preserved during the isomerization. Also note that one of the pyridyl groups that are *cis* (with respect to the 1,1′-biisoquinoline ligand) in the diastereomer on the left (bold rings) becomes *trans* in the diastereomer on the right. The other *cis* pyridyl group remains *cis*.

To distinguish between the irregular mechanisms that involve the breaking of Ru–N bonds and the regular mechanism that preserves them, we have determined the influence of acid on the rate of isomerization of **2**. The [H^+] is known to have a marked

(24) Hoskins, B. F.; Pannan, C. D. *J. Chem. Soc., Chem. Commun.* **1975**, 408.

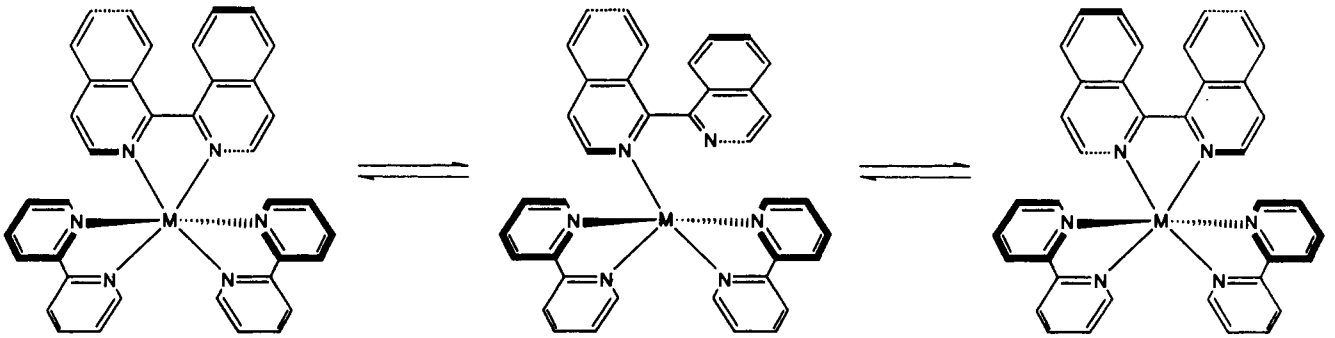

Figure 9. ~360° rotation about the σ bond of the η^1-1,1′-biiisoquinoline ligand. Note that the C_2 symmetry of the molecule and the *cis/trans* relationship of the 2,2′-bipyridine ligands are preserved during the isomerization.

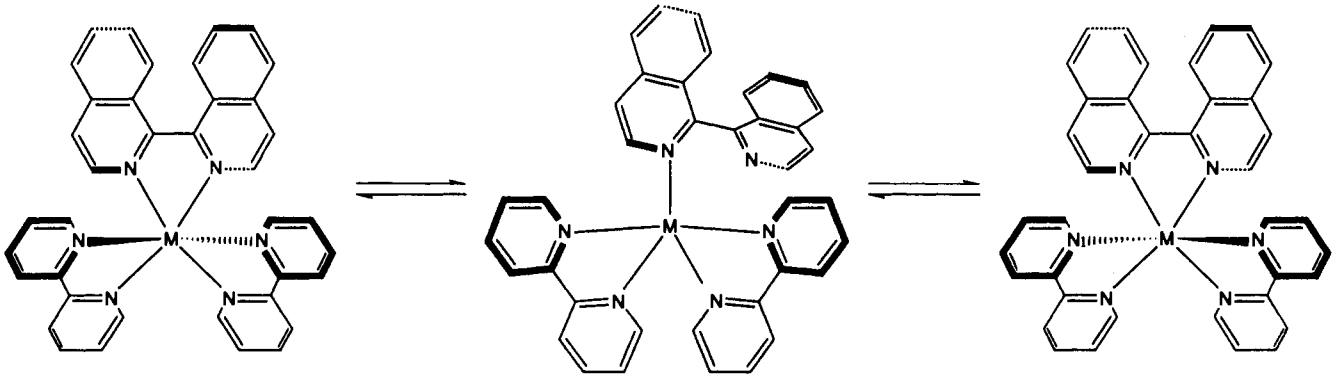

Figure 10. Turnstile rotation via a pentagonal-planar transition state. Note that the C_2 symmetry of the molecule and the *cis/trans* relationship of the 2,2′-bipyridine ligands are preserved during the isomerization.

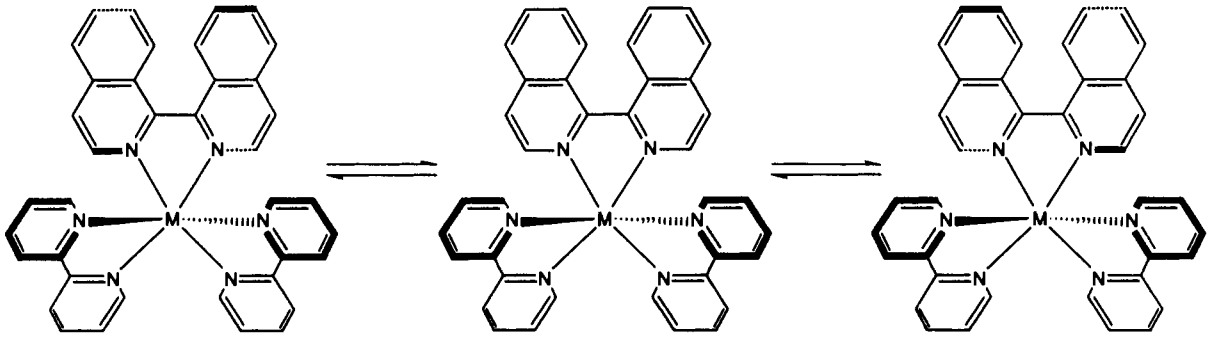

Figure 11. Isomerization via a planar η^2-1,1′-biiisoquinoline ligand. Note that the C_2 symmetry of the molecule and the *cis/trans* relationship of the 2,2′-bipyridine ligands are preserved during the isomerization. *This is the proposed mechanism.*

effect on the rates of racemization and ligand exchange of Δ/Λ-tris(2,2′-bipyridine)iron(II), which has been attributed to protonation of an η^1-2,2′-bipyridine ligand.[25] Unfortunately, the hexafluorophosphate salt of **2** is not water-soluble, but the chloride salt is. We have found the rate of isomerization of 15 mM D_2O solutions of Δ/Λ-(δ/λ-1,1′-biisoquinoline)bis(2,2′-bipyridine)-ruthenium(II) dichloride containing 1 M DCl (7.1(1) s^{-1} for maj→min) to be practically the same as that of solutions containing 1 M concentration of the electrolyte LiCl (5.7(2) s^{-1} for maj→min). The small difference in the rates may be attributed to differences in ion activity that are not readily quantified. Thus, the only mechanism that is consistent with all of the available kinetic and extrakinetic data is the third mechanism, isomerization of the ligand via a regular mechanism that involves a *syn* "planar" η^2-1,1′-biisoquinoline (Figure 11).

It is noteworthy that in its ground-state structure the σ-donor orbitals of the twisted 1,1′-biisoquinoline ligand are "misdirected" with respect to the σ-acceptor orbitals of the metal.[26] A planar 1,1′-biisoquinoline would direct the ligand's σ-donor orbitals toward the metal's σ-acceptor orbitals,[27] which could help overcome the energy required to bend the σ-bond of the 1,1′-biisoquinoline ligand sufficiently to allow H_8 and $H_{8'}$ to pass one another. In this regard, the strength of the kinetically inert Ru(II)–ligand bonds may actually facilitate the atropisomerization reaction. This hypothesis is currently being tested; we are measuring the rates of isomerization of the osmium derivative. The story appears to be a familiar one of a transition metal stabilizing a reactive organic moiety. In this case the species happens to be the transition state in the racemization of the chiral 1,1-biisoquinoline ligand.

Conclusion

We conclude that interconversion of the two diastereoisomers of **2** takes place by a regular mechanism that involves

(25) (a) Basolo, F.; Pearson, R. G. *Mechanisms of Inorganic Reactions*, 2nd ed.; John Wiley: New York, 1967; pp. 218, 219. (b) Baxendale, J. H.; George, P. *Trans. Faraday Soc.* **1950**, *46*, 736.

(26) Ashby, M. T.; Lichtenberger, D. L. *Inorg. Chem.* **1985**, *24*, 636.

(27) Ashby, M. T.; Enemark, J. H.; Lichtenberger, D. L.; Ortega, R. B. *Inorg. Chem.* **1986**, *25*, 3154.

atropisomerization of the η^2-1,1′-biisoquinoline ligand via a *syn* transition state. Thus while the free 1,1′-biisoquinoline presumably undergoes atropisomerization via an *anti* transition state, the *syn* pathway can be made facile upon coordination of the ligand. We believe the energy associated with deforming the binaphthyl skeleton is partially recovered when the misdirected nitrogen σ-donor orbitals of the 1,1′-biisoquinoline ligand are directed toward the ruthenium σ-acceptor orbitals in the planar transition state. It also seems likely that the unusual mechanism for isomerization of **2** is possible because a kinetically inert metal was employed. Accordingly, the strength of the Ru–N bonds both promotes the stabilization of the transition-state structure and insures that the Ru–N bonds remain intact during the isomerization process.[28,29]

Acknowledgment. We thank the donors of the Petroleum Research Fund, administered by the ACS, for partial support of this research. M.T.A. is grateful to the University of Oklahoma Research Council for a Junior Faculty Summer Research Fellowship. A.K.G. is grateful to the National Science Foundation for a Research Experience for Undergraduates fellowship. Drs. Bing Fung, Eric Enwall, and Steve Toth, Mr. Mathew Magnuson, and Mr. Collin Cross are thanked for their assistance with the NMR experiments. Mr. John Klaen is thanked for his contribution to the synthesis of 1,1′-biisoquinoline. The loan of ruthenium by the Johnson-Matthey Co. is gratefully acknowledged.

Supplementary Material Available: COSY spectrum of **2**; tables of positional parameters and thermal parameters for (Λ,λ)-**2** (7 pages). This material is contained in many libraries on microfiche, immediately follows this article in the microfilm version of the journal, and can be ordered from the ACS; see any current masthead page for ordering information.

(28) A referee has suggested that the facile atropisomerization of the 1,1′-biisoquinoline ligand of **2** relative to other 2-functionalized 1,1′-binaphthyl skeletons may be attributed to annulation of the five-membered heterometallacyle (cf.: Dore, A.; Fabbri, D.; Gladiali, S.; De Lucchi, O. *J. Chem. Soc., Chem. Commun.* **1993**, 1124). The angles about the C2 and C2′ carbon atoms of the 2,2′-bipyridine ligands suggest that the nitrogen atoms are somewhat pinched together upon coordination to the metal (the internal angles of a regular pentagon are 108°; N3–C19–C24 = 115.8(4)°, N4–C24–C19 = 115.4(4)°, N5–C29–C34 = 115.2(5)°, N6–C34–C29 = 115.6(4)°), and thus coordination of the 1,1′-biisoquinoline ligand and formation of a five-membered chelate ring (N1–C1–C10 = 113.2(4)°, N2–C10–C1 = 113.2(4)°) may reduce the transannular steric interaction between H_8 and $H_{8'}$. We intend to address the question of the relative importance of the chelate ring size and the "redirection" of the 1,1′-biisoquinoline ligand in future studies.

(29) An η^1-1,1′- biisoquinoline complex was known before this study (Dai, L.; Zhu, Z.; Zhang, Y.; Ni, C.; Zhang, Z.; Zhou, Y. *J. Chem. Soc., Chem. Commun.* **1987**, 1760). An η^2-1,1′-biisoquinoline complex was reported after this paper was submitted for review (Cheng, L.-K.; Yeung, K.-S.; Che, C.-M.; Cheng, M.-C.; Wang, Y. *Polyhedron* **1993**, *12*, 1201).